



ELSEVIER

Available online at [www.sciencedirect.com](http://www.sciencedirect.com)

SCIENCE @ DIRECT®

Nuclear Instruments and Methods in Physics Research A 538 (2005) 657–667

**NUCLEAR  
INSTRUMENTS  
& METHODS  
IN PHYSICS  
RESEARCH**  
Section A

[www.elsevier.com/locate/nima](http://www.elsevier.com/locate/nima)

# Scintillation properties and radioactive contamination of $\text{CaWO}_4$ crystal scintillators

Yu.G. Zdesenko<sup>a,\*</sup>, F.T. Avignone III<sup>b</sup>, V.B. Brudanin<sup>c</sup>, F.A. Danevich<sup>a,\*</sup>,  
S.S. Nagorny<sup>a</sup>, I.M. Solsky<sup>d</sup>, V.I. Tretyak<sup>a</sup>

<sup>a</sup>*Institute for Nuclear Research, Prospekt Nauki 47, MSP 03680 Kiev, Ukraine*

<sup>b</sup>*University of South Carolina, Columbia, South Carolina 29208, USA*

<sup>c</sup>*Joint Institute for Nuclear Research, 141980 Dubna, Russia*

<sup>d</sup>*Institute for Materials, 79031 Lviv, Ukraine*

Received 11 March 2004; received in revised form 2 September 2004; accepted 16 September 2004

Available online 30 October 2004

## Abstract

Energy resolution,  $\alpha/\beta$  ratio and the pulse-shape discrimination ability of the  $\text{CaWO}_4$  crystal scintillators were studied. The radioactive contamination and background of the crystals were measured in the Solotvina Underground Laboratory. Despite a rather high level of radioactive impurities, the background rate of the  $\text{CaWO}_4$  detector in the energy window of the  $^{48}\text{Ca}$  neutrinoless  $2\beta$  decay (3.6–5.4 MeV) was reduced to 0.07 counts/(yr keV kg). The indication for  $\alpha$  decay of  $^{180}\text{W}$  (Phys. Rev. 67 (2003) 014310) was confirmed (the measured half-life is  $T_{1/2} = 1.0_{-0.3}^{+0.7} \times 10^{18}$  yr). © 2004 Elsevier B.V. All rights reserved.

PACS: 29.40.Mc; 23.60.+e; 23.40.-s; 95.35.+d

Keywords: Scintillation detector;  $\text{CaWO}_4$  crystals; Alpha decay; Double beta decay; Dark matter

## 1. Introduction

The energy resolution, pulse-shape discrimination ability, and radioactive purity of the detectors are very important in experiments aiming to search for the neutrinoless double beta ( $0\nu 2\beta$ ) decay of

atomic nuclei (see reviews [1–4]), and to search for weakly interacting massive particles (so-called WIMPs)<sup>1</sup> as a possible component of the dark matter in the Universe [5].

<sup>1</sup>Weakly interacting massive particles (WIMPs)—in particular the neutralino, predicted by the minimal supersymmetric extension of the SM—are considered as possible component of the dark matter in the Universe. It is assumed that WIMPs interact with matter through scattering on nuclei, and hence, produce low energy nuclear recoils. At present the most

\*Corresponding author. Tel.: +380 44 265 1111; fax: +380 44 265 4463.

E-mail address: [danevich@kinr.kiev.ua](mailto:danevich@kinr.kiev.ua) (F.A. Danevich).

\*Deceased

Because the theoretical  $0\nu2\beta$  decay rate strongly depends on the  $Q_{\beta\beta}$ -value, roughly as  $Q_{\beta\beta}^5$  [6], the development of new low-background detectors, containing potentially  $2\beta$  decaying nuclides with a  $Q_{\beta\beta}$  energy release as large as possible, is very important. As  $^{48}\text{Ca}$  has the highest  $Q_{\beta\beta}$  energy among 35 double  $\beta^-$  decay candidates available in nature, a detector containing Ca nuclei would be of considerable interest for the future high sensitivity  $2\beta$  decay experiments. However, apart from a reasonable content of candidate nuclei, a detector for  $2\beta$  study should satisfy certain demands on its radiopurity, because the latter governs the level of residual detector background. In addition, the energy resolution of the detector is extremely important. Most important, good energy resolution minimizes the irreducible background produced by  $2\nu2\beta$  decay events. Likewise, the role of the detector's energy resolution is even more crucial for the discovery of  $0\nu2\beta$  decay. Indeed, this process manifests itself through a peak at the  $Q_{\beta\beta}$  energy, the width of which is determined by the energy resolution of the detector. Hence, the latter should be sufficient to discriminate this peak from background and to recognize the effect [7]. One possible detector for the  $2\beta$  decay study of  $^{48}\text{Ca}$  is the calcium tungstate ( $\text{CaWO}_4$ ) crystal scintillator, the physical properties of which are similar to those of the  $\text{CdWO}_4$  scintillator already applied in a  $2\beta$  experiment with  $^{116}\text{Cd}$  [8].

Moreover, in Refs. [9,10]  $\text{CaWO}_4$  crystals are discussed as very promising detectors for dark matter particle searches. However, because of an extremely low counting rate expected from WIMP scattering by nuclei, such measurements require detectors with extremely low levels of background [5].

The aim of this work is the study of the scintillation properties and radioactive contaminations of  $\text{CaWO}_4$  crystals and, on this basis to discuss the possible development of detectors for double beta decay and dark matter experiments.

(footnote continued)

sensitive experiments for WIMP searches use a range of detectors: Ge semiconductor detectors, low temperature bolometers, and scintillators [5].

## 2. Measurements and results

### 2.1. Scintillation properties of $\text{CaWO}_4$ crystals

$\text{CaWO}_4$  single crystals were discovered as being scintillators more than fifty years ago [11,12]. Beard and Kelly used a small  $\text{CaWO}_4$  crystal in a low background experiment to search for alpha activity in natural tungsten [13]. The main properties of the  $\text{CaWO}_4$  scintillators are presented in Table 1, where the characteristics of cadmium tungstate ( $\text{CdWO}_4$ ) crystals are given for comparison. Both crystals are chemically resistant, while  $\text{CaWO}_4$  possesses better mechanical properties.

For our studies, three clear colorless  $\text{CaWO}_4$  crystals (20 mm × 20 mm × 10 mm, 40 mm × 34 mm × 23 mm, and  $\varnothing$ 40 mm × 39 mm) were grown by the Czochralski method. These crystals, wrapped in PTFE reflector tape, were optically coupled to 3 in. Philips XP2412 photomultipliers (PMTs). The event-by-event data acquisition records information on the amplitude (energy), arrival time and pulse shape of the signals. For the latter a transient digitizer based on a fast 12 bit ADC (AD9022) was used with a sampling frequency of 20 MHz. Pulse shapes of events in the chosen energy interval (usually, higher than  $\approx 180$  keV) were recorded in 2048 channels with 50 ns channel's width.

The linearity, energy scale and resolution of the detector were measured with  $\gamma$ -ray sources of  $^{60}\text{Co}$ ,  $^{137}\text{Cs}$ ,  $^{207}\text{Bi}$ ,  $^{232}\text{Th}$  and  $^{241}\text{Am}$  in the energy range

Table 1  
Properties of  $\text{CaWO}_4$  and  $\text{CdWO}_4$  crystal scintillators

Properties	$\text{CaWO}_4$	$\text{CdWO}_4$
Density (g/cm <sup>3</sup> )	6.1	8.0
Melting point (°C)	1570–1650	1325
Structural type	Sheelite	Wolframite
Cleavage plane	Weak (101)	Marked (010)
Hardness (Mohs)	4.5–5	4–4.5
Wavelength of emission maximum (nm)	420–425	480
Refractive index	1.94	2.2–2.3
Effective average decay time ( $\mu\text{s}$ ) <sup>a</sup>	8	13
Relative light output <sup>a</sup>	90%	100%

<sup>a</sup>For  $\gamma$  rays at 20 °C.

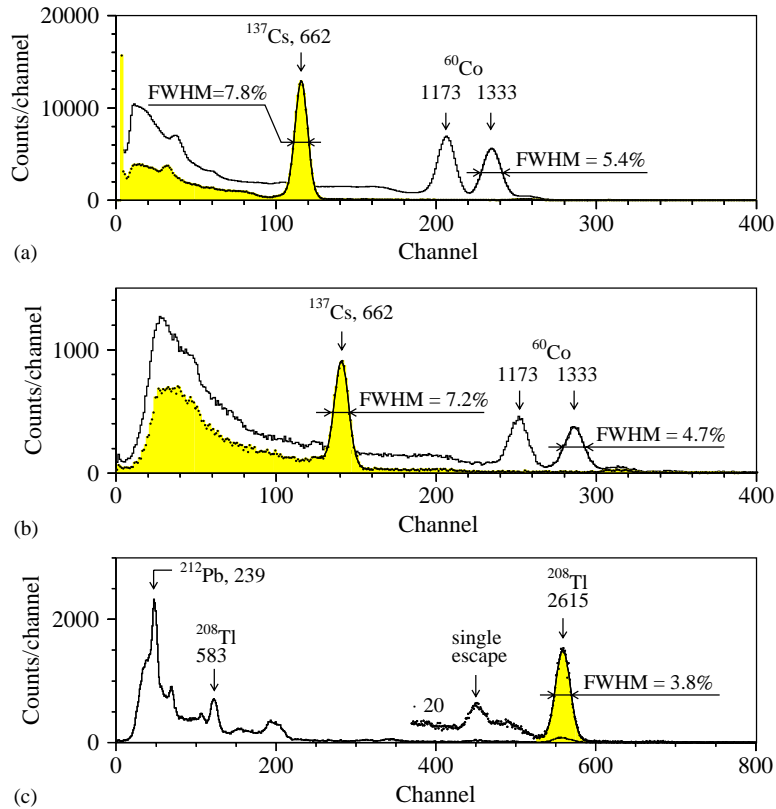


Fig. 1. Energy spectra of the  $^{137}\text{Cs}$  and  $^{60}\text{Co}$  gamma sources measured with the  $\text{CaWO}_4$  scintillation crystal ( $\varnothing 40\text{ mm} \times 39\text{ mm}$ ) in two detector arrangements (with different conditions of the light collection): (a) standard, where the crystal, wrapped in PTFE reflector tape, was optically coupled to the PMT; (b) the  $\text{CaWO}_4$  crystal was located in a liquid and viewed by two distant PMTs. (c) The same as (b) but with the  $^{232}\text{Th}$  gamma source.

of 60–2615 keV. Fig. 1(a) shows the energy spectra of the  $^{137}\text{Cs}$  and  $^{60}\text{Co}$   $\gamma$ -rays measured with a crystal of dimensions  $\varnothing 40\text{ mm} \times 39\text{ mm}$ . For example, the energy resolution,  $\text{FWHM} = 7.8\%$  at 662 keV, is comparable with that of  $\text{NaI}(\text{Tl})$  scintillators.

Moreover, a further improvement of the energy resolution was achieved by placing the  $\text{CaWO}_4$  crystal ( $\varnothing 40\text{ mm} \times 39\text{ mm}$ ) in a liquid (silicone oil). The crystal was fixed in the center of a teflon container with inner diameter 70 mm, which was coupled on opposite sides with two PMTs Philips XP2412. The container was filled up with pure and transparent silicon oil (refractive index  $\approx 1.5$ ). The spectra measured with the  $^{60}\text{Co}$ ,  $^{137}\text{Cs}$  and  $^{232}\text{Th}$   $\gamma$  sources are shown in Fig. 1(b) and (c). By comparing the spectra in Fig. 1(a) and (b), one

finds that an increase in light collection of  $\approx 20\%$  was reached with the  $\text{CaWO}_4$  crystal placed in the liquid. It resulted in an improvement of the energy resolution over the entire energy region: the measured FWHM resolution is equal to 7.2%, 4.7% and 3.8% for 662, 1333 and 2615 keV  $\gamma$ -ray lines, respectively (see Fig. 1(b) and (c)).

The detector response to  $\alpha$  particles in the energy range of 0.5–5.3 MeV was measured with the help of a collimated beam of  $\alpha$  particles<sup>2</sup> from an  $^{241}\text{Am}$  source and using various sets of the thin

<sup>2</sup>The  $\text{CaWO}_4$  crystals were irradiated in the directions perpendicular to main crystal planes with the aim to check a possible dependence of the  $\alpha$  signal on the direction of irradiation. While earlier such a dependence has been found for  $\text{CdWO}_4$  [14], we did not observe it for the  $\text{CaWO}_4$  crystals.

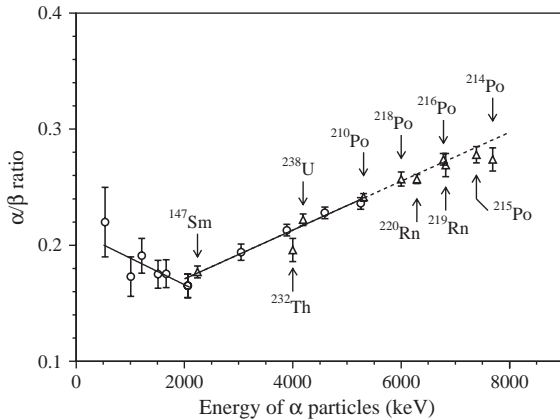


Fig. 2. The energy dependence of the  $\alpha/\beta$  ratio measured with the 40 mm  $\times$  34 mm  $\times$  23 mm  $\text{CaWO}_4$  scintillator. The crystal was irradiated by  $\alpha$  particles ( $^{241}\text{Am}$ ) through absorbers to obtain energies in the 0.5–5.3 MeV range (circles). In addition, the  $\alpha$  peaks of  $^{147}\text{Sm}$ , as well as  $^{232}\text{Th}$ ,  $^{238}\text{U}$ , and  $^{235}\text{U}$  daughters (triangles) were selected from the background data with the help of pulse-shape and time-amplitude analyses (see text). Solid lines represent the best fit for the  $\alpha/\beta$  ratio in two energy intervals: 0.5–2 MeV and 2–5.3 MeV.

mylar film absorbers. The energies of the  $\alpha$  particles after the absorbers were measured with a surface-barrier detector (see for details [14]). In addition,  $\alpha$  peaks of the  $^{147}\text{Sm}$  and nuclides from the  $^{232}\text{Th}$ ,  $^{235}\text{U}$  and  $^{238}\text{U}$  chains, present in trace amounts in the  $\text{CaWO}_4$  crystal (40 mm  $\times$  34 mm  $\times$  23 mm), were used to extend the energy interval up to  $\simeq 8$  MeV. These peaks were selected with the help of pulse-shape and time-amplitude analyses of the data obtained in the low background measurements with the  $\text{CaWO}_4$  crystal (see section 2.3). The energy dependence of the  $\alpha/\beta$  ratio is presented in Fig. 2. Within the energy interval 0.5–2 MeV, the measured  $\alpha/\beta$  ratio<sup>3</sup> decreases with increasing energy as  $\alpha/\beta = 0.21(2) - 0.023(14)E_\alpha$ , while above 2 MeV it increases as  $\alpha/\beta = 0.129(12) + 0.021(3)E_\alpha$  ( $E_\alpha$  is in MeV). The quenching of the scintillation light caused by  $\alpha$  particles in comparison with electrons is due to the

<sup>3</sup>The “ $\alpha/\beta$  ratio” is defined as the ratio of the  $\alpha$  peak position measured in the  $\gamma$  energy scale to the energy of the  $\alpha$  particles. As  $\gamma$  quanta interact with the detector via  $\beta$  particles we use the more convenient term “ $\alpha/\beta$  ratio”.

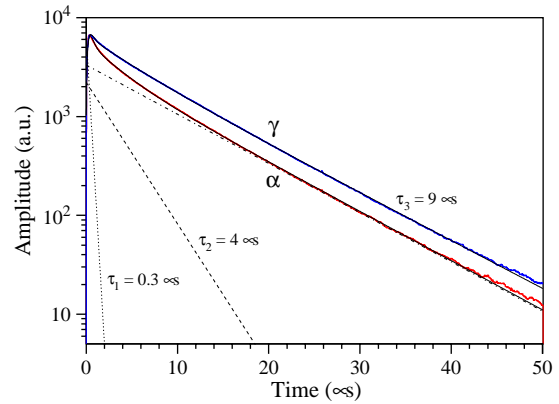


Fig. 3. Shapes of scintillation pulses in the  $\text{CaWO}_4$  crystals for  $\gamma$  rays and  $\alpha$  particles (each was obtained as the average of 4000 pulses) and their fit by three exponential functions with decay constants  $\approx 0.3 \mu\text{s}$ ,  $\approx 4 \mu\text{s}$  and  $\approx 9 \mu\text{s}$ .

higher ionization density of  $\alpha$  particles [15]. This behavior of the  $\alpha/\beta$  ratio can then be explained by the energy dependence of the ionization density of  $\alpha$  particles.

## 2.2. Pulse-shape analysis

The time characteristics of  $\text{CaWO}_4$  scintillators were studied as described in [14,16] with the help of a transient digitizer based on a 12 bit ADC operated at a sampling frequency of 20 MHz. Shapes (time dependence) of the light pulses produced by  $\alpha$  particles and  $\gamma$  rays in  $\text{CaWO}_4$  scintillator are depicted in Fig. 3 (shown is the average of 4000 shapes). These shapes were fit with the function:  $f(t) = \sum A_i/(\tau_i - \tau_0) \times (e^{-t/\tau_i} - e^{-t/\tau_0})$ , where  $A_i$  are intensities (in percentage of the total intensity),  $\tau_0 \approx 0.2 \mu\text{s}$  is the integration constant of the electronics, and  $\tau_i$  are decay constants for different light emission components. The best fit was achieved with three<sup>4</sup> decay components ( $\tau_i \approx 0.3$ ,  $\approx 4$  and  $\approx 9 \mu\text{s}$ ) with different intensities for  $\gamma$  rays and  $\alpha$  particles (see Table 2).

<sup>4</sup>In principle, a reasonable fit has also been obtained by using only two components:  $\approx 2 \mu\text{s}$  and  $\approx 9 \mu\text{s}$ . However, in order to reproduce the shape at the beginning of the pulses one more component ( $\approx 0.3 \mu\text{s}$ ) must be added.

Table 2

Decay time of CaWO<sub>4</sub> scintillators for  $\gamma$  quanta and  $\alpha$  particles at 20°C. The decay constants and their intensities (in percentage of the total intensity) are denoted as  $\tau_i$  and  $A_i$ , respectively

Type of irradiation	Decay constants, $\mu$ s		
	$\tau_1$ ( $A_1$ )	$\tau_2$ ( $A_2$ )	$\tau_3$ ( $A_3$ )
$\gamma$ rays	0.3 (3%)	4.4 (15%)	9.0 (82%)
$\alpha$ particles	0.3 (6%)	3.2 (18%)	8.8 (76%)

This difference allows one to discriminate  $\gamma(\beta)$  events from those of  $\alpha$  particles. For this the optimal filter method was used (for the first time proposed in [17]), which previously was successfully applied to CdWO<sub>4</sub> scintillators [16]. To obtain the numerical characteristics of CaWO<sub>4</sub> signals, called the shape indicator (SI), each experimental pulse,  $f(t)$ , was processed with the following digital filter:  $SI = \sum f(t_k) \times P(t_k) / \sum f(t_k)$ , where the sum is over time channels  $k$ , starting from the origin of pulse and up to 75  $\mu$ s, and  $f(t_k)$  is the digitized amplitude (at the time  $t_k$ ) of a given signal. The weight function  $P(t)$  is defined as:  $P(t) = \{\bar{f}_\alpha(t) - \bar{f}_\gamma(t)\} / \{\bar{f}_\alpha(t) + \bar{f}_\gamma(t)\}$ , where  $\bar{f}_\alpha(t)$  and  $\bar{f}_\gamma(t)$  are the reference pulse shapes for  $\alpha$  particles and  $\gamma$  quanta, respectively, resulting from the average of a large number of experimental pulse shapes.

As an example, the SI distributions measured with the CaWO<sub>4</sub> scintillator with  $\alpha$  particles ( $E_\alpha \approx 5.3$  MeV) and  $\gamma$  quanta ( $\approx 1.2$  MeV) are shown in Fig. 4(a), from which one can see that by using this approach, a distinct discrimination between  $\alpha$  particles and  $\gamma$  rays ( $\beta$  particles) was achieved. As a measure of discrimination ability, the following relation can be used:  $M_{PSA} = |SI_\alpha -$

$SI_\gamma| / \sqrt{\sigma_\alpha^2 + \sigma_\gamma^2}$ , where  $SI_\alpha$  and  $SI_\gamma$  are mean SI values for  $\alpha$  particles and  $\gamma$  quanta distributions (which are well described by Gaussian functions), where  $\sigma_\alpha$  and  $\sigma_\gamma$  are the corresponding standard deviations. For the distributions presented in Fig. 4(a),  $M_{PSA} = 5.9$ .

The energy dependence of the SI was studied in the energy region 1–5.3 MeV for alpha particles (see Fig. 4(b)) and 0.1–2.6 MeV for gamma

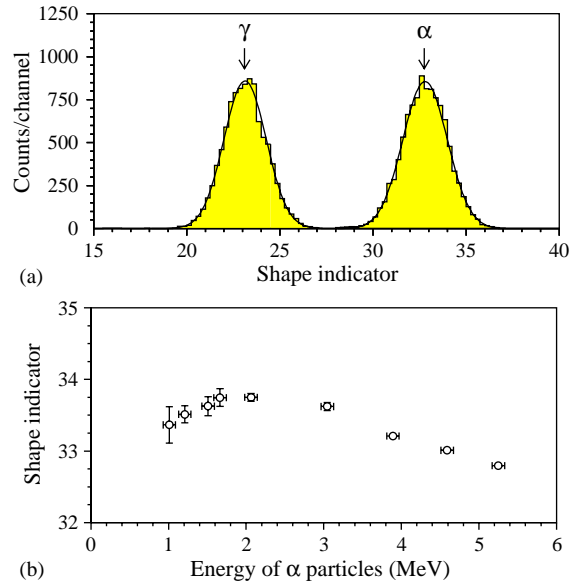


Fig. 4. (a) The shape indicator (see text) distributions measured with the CaWO<sub>4</sub> detectors with the  $\alpha$  particles ( $E_\alpha = 5.3$  MeV) and  $\gamma$  quanta ( $\approx 1.2$  MeV). (b) The energy dependence of the shape indicator measured with the CaWO<sub>4</sub> crystal scintillator for  $\alpha$  particles.

quanta. Like the  $\alpha/\beta$  ratio, the energy dependence of the shape indicator for  $\alpha$  particles (see Fig. 4(b)) can be explained by the dependence of the ionization density on the energy (note that the higher SI value corresponds to the shorter decay time of scintillation pulses). The shape indicator measured with CaWO<sub>4</sub> crystals for  $\alpha$  particles does not depend on the direction of  $\alpha$  irradiation relative to the crystal axes. Similarly, no dependence of the SI on the  $\gamma$  quanta energy (from 0.1 to 2.6 MeV) was observed.

### 2.3. Radioactive contamination

The radioactive contamination of the crystals was measured in the low background set-up installed in the Solotvina Underground Laboratory built in a salt mine 430 m underground ( $\approx 1000$  m of water equivalent) [18]. In the set-up a CaWO<sub>4</sub> crystal scintillator (40 mm  $\times$  34 mm  $\times$  23 mm) was coupled to a special low-radioactive 5 in.-photomultiplier tube (EMI D724KFLB) with a quartz light-guide  $\varnothing 10$  cm  $\times$  33 cm. The

detector was surrounded by a passive shield made of teflon (thickness of 3–5 cm), plexiglass (6–13 cm), high purity (HP) copper (3–6 cm), lead (15 cm) and polyethylene (8 cm). Two plastic scintillators (120 cm × 130 cm × 3 cm) were installed above the passive shield and used as a cosmic muon veto. For each event in the detector, the amplitude of the signal and its arrival time were recorded. In addition the  $\text{CaWO}_4$  scintillation pulses were digitized with a 20 MHz sampling frequency over  $\approx 100 \mu\text{s}$  time interval. The energy resolution of the detector was determined by calibrations with  $^{60}\text{Co}$ ,  $^{137}\text{Cs}$ ,  $^{207}\text{Bi}$  and  $^{232}\text{Th}$   $\gamma$  sources. In the energy range 240–2615 keV, it can be fit by the function:  $\text{FWHM}_\gamma(\text{keV}) = -3 + \sqrt{6.9E_\gamma}$ , where  $E_\gamma$  is the energy of  $\gamma$ -ray in keV. Routine calibrations were carried out weekly with  $^{207}\text{Bi}$  and  $^{232}\text{Th}$   $\gamma$  sources.

The energy spectrum of the  $\text{CaWO}_4$  detector, measured during 1734 h in the low background apparatus, is presented in Fig. 5, where the data obtained with the  $\text{CdWO}_4$  scintillator in the same set-up are shown for comparison. Both spectra are normalized by their measuring times and their corresponding detector masses. It is clear from this comparison, that the radioactive contamination of the  $\text{CaWO}_4$  crystal is much higher than that of the  $\text{CdWO}_4$ . With the aim of recognizing the origins of

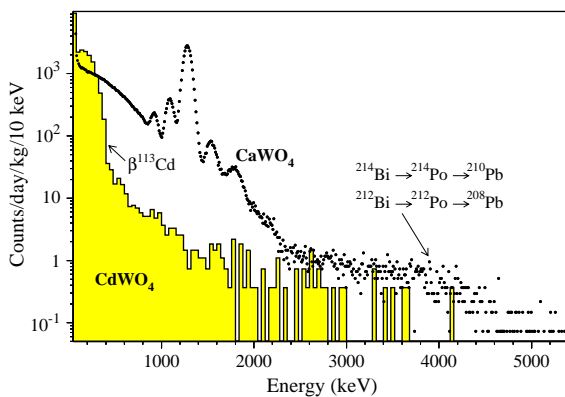


Fig. 5. Energy spectra of  $\text{CaWO}_4$  (189 g, 1734 h, dots), and  $\text{CdWO}_4$  (448 g, 37 h, histogram) scintillation crystals measured in the same low background set-up. The  $\text{CaWO}_4$  detector is considerably contaminated by radionuclides from the U–Th chains. Beta decay of  $^{113}\text{Cd}$  ( $Q_\beta = 316 \text{ keV}$ ,  $T_{1/2} = 7.7 \times 10^{15} \text{ yr}$ ) dominates in the low energy part of the  $\text{CdWO}_4$  spectrum.

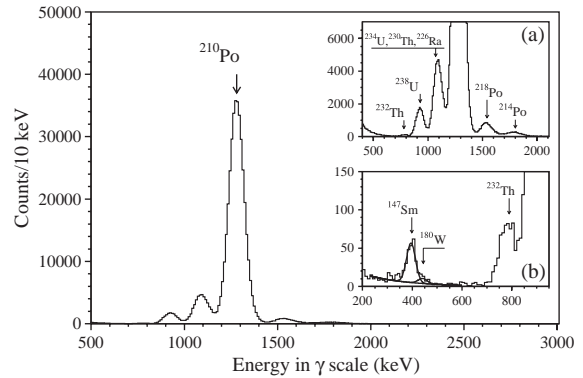


Fig. 6. Background  $\alpha$  spectrum of the  $\text{CaWO}_4$  detector (189 g, 1734 h) selected with the help of the pulse-shape analysis. (Inset a) The energy distribution of  $\alpha$  particles is well reproduced by the model which includes  $\alpha$  decays of nuclides from  $^{232}\text{Th}$  and  $^{238}\text{U}$  families. (Inset b) Low energy part of the  $\alpha$  spectrum. The peculiarity on the right of the  $^{147}\text{Sm}$  peak can be attributed to the  $\alpha$  decay of  $^{180}\text{W}$  with  $T_{1/2} = 1.0 \times 10^{18} \text{ yr}$ .

these contaminations, the data accumulated with the  $\text{CaWO}_4$  crystal were separated into  $\alpha$  and  $\beta$  spectra with the help of the pulse-shape discrimination technique.

The  $\alpha$  spectrum, which is depicted in Fig. 6, was analyzed. The total alpha activity in the calcium tungstate crystal is  $\approx 0.4 \text{ Bq/kg}$ . The intense clear peak at the energy of 1.28 MeV is attributed to intrinsic  $^{210}\text{Po}$  (daughter of  $^{210}\text{Pb}$  from the  $^{238}\text{U}$  family) with an activity of 0.291(5) Bq/kg. Apparently, the equilibrium of the uranium chain in the crystal was broken during crystal production, because the peak of  $^{238}\text{U}$  (see inset (a) in Fig. 6) corresponds to a much lower activity of 14.0(5) mBq/kg.

The alpha peaks of the uranium daughters  $^{234}\text{U}$ ,  $^{230}\text{Th}$ ,  $^{226}\text{Ra}$  are not resolved (their  $Q_\alpha$  values are very close), however, the area of the total peak (at  $\approx 1.1 \text{ MeV}$ ) is in satisfactory agreement with the activity of  $^{238}\text{U}$  and  $^{226}\text{Ra}$ . Another member of the family,  $^{222}\text{Rn}$ , is not separated from  $^{210}\text{Po}$  (the expected energy of the  $\alpha$  peak is  $\approx 1.34 \text{ MeV}$  in  $\gamma$ -ray energy), while the  $^{218}\text{Po}$  peak is well resolved. The activity of  $^{226}\text{Ra}$  determined on the basis of the  $^{218}\text{Po}$  peak area is 5.9(8) mBq/kg.

In the low energy part of the alpha spectrum (inset (b) in Fig. 6) the peak at  $\approx 0.8 \text{ MeV}$  can be attributed to  $^{232}\text{Th}$  with an activity of

0.69(10) mBq/kg. A weak alpha peak with the  $\gamma$ -equivalent energy of 395(2) keV (corresponds to the energy of  $\alpha$  particles, 2243(9) keV) can be explained by traces of  $^{147}\text{Sm}$  ( $E_\alpha = 2247$  keV,  $T_{1/2} = 1.06 \times 10^{11}$  yr, the natural isotopic abundance of which is 15.0% [19]) with an activity 0.49(4) mBq/kg.<sup>5</sup>

In addition, the raw background data (Fig. 5) were analyzed using the time-amplitude method, where the energy and arrival time of each event were used for the selection of the decay chains of the  $^{232}\text{Th}$ ,  $^{235}\text{U}$  and  $^{238}\text{U}$  families.<sup>6</sup> For instance, the following sequence of  $\alpha$  decays from the  $^{232}\text{Th}$  family was searched for and observed:  $^{220}\text{Rn}$  ( $Q_\alpha = 6.41$  MeV,  $T_{1/2} = 55.6$  s)  $\rightarrow$   $^{216}\text{Po}$  ( $Q_\alpha = 6.91$  MeV,  $T_{1/2} = 0.145$  s)  $\rightarrow$   $^{212}\text{Pb}$  (which are in equilibrium with  $^{228}\text{Th}$ ). Since the energy of  $\alpha$  particles from the  $^{220}\text{Rn}$  decay corresponds to  $\approx 1.6$  MeV in  $\gamma$ -ray energy in the  $\text{CaWO}_4$  detector, events in the energy region 1.4–2.2 MeV were used as triggers. Then all events (within 1.4–2.2 MeV) following the triggers in the time interval 20–600 ms (containing 85.2% of  $^{216}\text{Po}$  decays) were selected. The obtained  $\alpha$  peaks (see Fig. 7)—the  $\alpha$  nature of events was confirmed by the pulse-shape analysis described above—as well as the distributions of the time intervals between events are in a good agreement with those expected for the  $\alpha$ -decays of the  $^{220}\text{Rn} \rightarrow ^{216}\text{Po} \rightarrow ^{212}\text{Pb}$  chain [20]. On this basis, the activity of  $^{228}\text{Th}$  in the  $\text{CaWO}_4$  crystal was calculated as 0.6(2) mBq/kg, which is in good agreement with the activity of  $^{232}\text{Th}$  (0.69(10) mBq/kg) determined from the  $\alpha$  spectrum. The  $\alpha$  peak with energy  $E_\alpha \approx 7.3$  MeV, which is present in the energy distribution of the second event in Fig. 7, can be attributed to  $^{215}\text{Po}$  ( $Q_\alpha = 7.39$  MeV,  $T_{1/2} = 1.78$  ms) in the  $^{235}\text{U}$  chain. The corresponding activity of  $^{227}\text{Ac}$  in the crystal is 1.6(3) mBq/kg. Again we have to conclude that the equilibrium of the  $^{235}\text{U}$  chain in the crystal is also broken. Indeed, because the uranium isotopes  $^{238}\text{U}$ ,

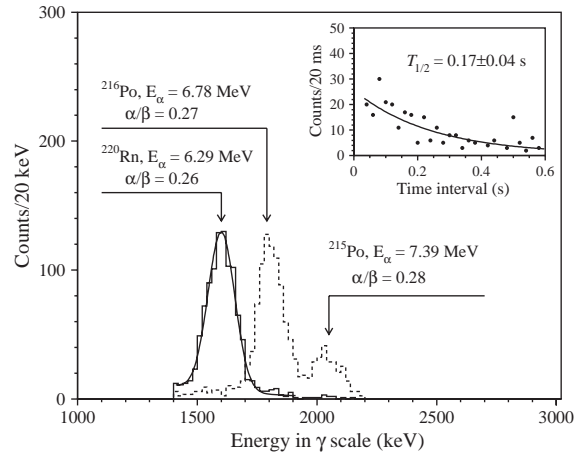


Fig. 7. Alpha peaks of  $^{220}\text{Rn}$  and  $^{216}\text{Po}$  selected by the time-amplitude analysis from the data accumulated with the  $\text{CaWO}_4$  detector. (Inset) The time distribution between the first and second events together with an exponential fit. The obtained half-life of  $^{216}\text{Po}$  ( $0.17 \pm 0.04$  s) agrees with the table value ( $0.145 \pm 0.002$  s) [20].

$^{234}\text{U}$  and  $^{235}\text{U}$  cannot be chemically separated, their activities have to be in the ratio 1 : 1 : 0.046, which leads to expected activity of  $^{235}\text{U}$  and its daughters of 0.64(2) mBq/kg.

Similarly for the analysis of the  $^{226}\text{Ra}$  chain ( $^{238}\text{U}$  chain) the following sequence of  $\beta$  and  $\alpha$  decays was used:  $^{214}\text{Bi}$  ( $Q_\beta = 3.27$  MeV)  $\rightarrow$   $^{214}\text{Po}$  ( $Q_\alpha = 7.83$  MeV,  $T_{1/2} = 164$   $\mu\text{s}$ )  $\rightarrow$   $^{210}\text{Pb}$ . For the first event, the lower energy threshold was set at 0.18 MeV, while for the second decay the energy window 1.6–2.4 MeV was chosen. A time interval of 90–500  $\mu\text{s}$  (56% of  $^{214}\text{Po}$  decays) was used. The obtained spectra (Fig. 8) lead to a  $^{226}\text{Ra}$  activity in the  $\text{CaWO}_4$  crystal of 5.6(5) mBq/kg, which agrees with the value derived on the basis of the  $^{218}\text{Po}$  peak in the  $\alpha$  spectrum.

In the beta spectrum of  $^{214}\text{Bi}$  (Fig. 8) there is a peak at  $\approx 1.8$  MeV which can be attributed to the  $\alpha$  decay of  $^{219}\text{Rn}$  ( $^{235}\text{U}$  family,  $E_\alpha = 6.82$  MeV,  $T_{1/2} = 3.96$  s). It was shown by pulse-shape analysis that this peak consists of  $\alpha$  events. The alpha peak of  $^{215}\text{Po}$  ( $E_\alpha = 7.39$  MeV) is not resolved from that of  $^{214}\text{Po}$ . The corresponding activity of  $^{227}\text{Ac}$  in the crystal is 1.6(3) mBq/kg;

<sup>5</sup>The presence of  $^{147}\text{Sm}$  in a  $\text{CaWO}_4$  crystal (at a level of  $\approx 6$  mBq/kg) was also observed in Ref. [10], where this crystal was used as a low temperature bolometer with very good energy resolution for alpha particles.

<sup>6</sup>The technique of time-amplitude analysis of background data to recognize the presence of the short-living chains from  $^{232}\text{Th}$ ,  $^{235}\text{U}$  and  $^{238}\text{U}$  families is described in Refs. [21,22].

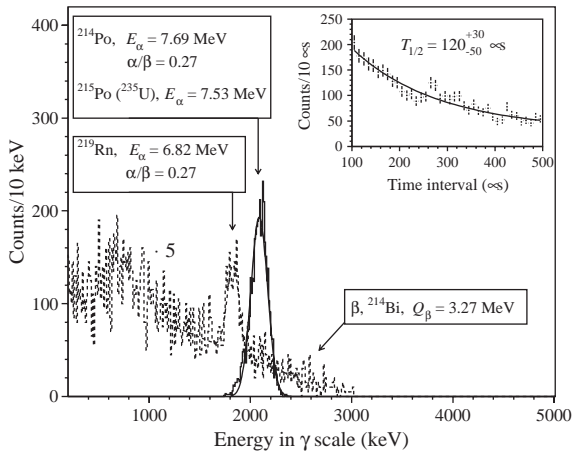


Fig. 8. The energy distributions for the fast sequence of the  $\beta$  ( $^{214}\text{Bi}$ ) and  $\alpha$  ( $^{214}\text{Po}$ ) decays selected from the background data by the time-amplitude analysis. The peak in the continuous spectrum corresponds to the  $\alpha$  peak of  $^{219}\text{Rn}$  ( $E_\alpha \approx 6.82$  MeV) from the  $^{235}\text{U}$  chain. (Inset) The time distribution between the first and second events together with an exponential fit (the contribution from  $^{215}\text{Po}$  was taken into account). The obtained half-life of  $^{214}\text{Po}$  ( $120_{-50}^{+30}$   $\mu\text{s}$ ) is in agreement with the table value ( $164.3 \pm 2$ )  $\mu\text{s}$  [20].

this value agrees with that determined by the time-amplitude analysis (see Fig. 7).

Finally, we analyze the energy spectrum of  $\beta(\gamma)$  events selected with the help of the pulse-shape technique and presented in Fig. 9. The background in the very low energy part of the  $\beta$  spectrum (see inset in Fig. 9) is mainly due to the  $\beta$  decay of  $^{210}\text{Pb}$  ( $Q_\beta = 64$  keV), whose measured activity is consistent with that determined from the  $\alpha$  peak of  $^{210}\text{Po}$ . The counting rate for the  $\beta(\gamma)$  spectrum above 0.2 MeV is  $\approx 0.45$  counts/(s kg). The contribution of the external  $\gamma$  rays to this background rate was estimated to be as small as  $\approx 2\%$ , by using the results of measurements with a  $\text{CdWO}_4$  crystal (mass of 0.448 kg) installed in the same low background set-up (see Fig. 5).

Therefore, the remaining  $\beta(\gamma)$  events are caused by the intrinsic contaminations of the  $\text{CaWO}_4$  crystal. The major part of this  $\beta$  activity can be ascribed to:  $^{210}\text{Bi}$ , daughter of  $^{210}\text{Pb}$  ( $\approx 0.3$  Bq/kg);  $^{234m}\text{Pa}$  ( $\approx 14$  mBq/kg);  $^{214}\text{Pb}$  and  $^{214}\text{Bi}$  from  $^{238}\text{U}$  family ( $\approx 9$  mBq/kg);  $^{211}\text{Pb}$  from  $^{235}\text{U}$  chain ( $\approx 2$  mBq/kg). The residual

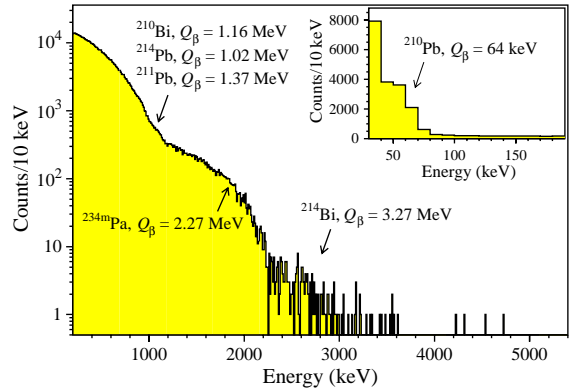


Fig. 9. Energy spectrum of the  $\beta(\gamma)$  events selected by the pulse-shape analysis technique from the background data measured during 1734 h with the  $\text{CaWO}_4$  detector. The distribution is described by the  $\beta$  spectra of  $^{210}\text{Bi}$ ,  $^{214}\text{Pb}$ ,  $^{211}\text{Pb}$ ,  $^{234m}\text{Pa}$ , and  $^{214}\text{Bi}$ . (Inset) In the low energy region, the background (measured during 15.8 h) is caused mainly by  $\beta$  decay of  $^{210}\text{Pb}$ .

( $\approx 0.13$  Bq/kg) can be explained by larger activity of  $^{210}\text{Bi}$  (assuming broken equilibrium in the  $^{210}\text{Bi} \rightarrow ^{210}\text{Po}$  chain), and/or by the presence of other  $\beta$  active impurities ( $^{40}\text{K}$ ,  $^{90}\text{Sr}$ ,  $^{137}\text{Cs}$ ) in the crystal.

In the high energy region of the  $\beta(\gamma)$  spectrum (3.6–5.4 MeV), which is the region of main interest in the search for the  $0\nu 2\beta$  decay of  $^{48}\text{Ca}$ , there are only 5 background counts. At the same time, in the same energy interval of initial spectrum (Fig. 5), there exists a broad distribution. It can be attributed to: (i) the  $\beta \rightarrow \alpha$  decays of  $^{214}\text{Bi} \rightarrow ^{214}\text{Po} \rightarrow ^{208}\text{Pb}$  ( $^{238}\text{U}$  chain). These events were tagged by the time-amplitude and pulse-shape discrimination techniques as described above; (ii) the fast  $\beta \rightarrow \alpha$  sequence of  $^{212}\text{Bi}$  ( $Q_\beta = 2254$  keV)  $\rightarrow ^{212}\text{Po}$  ( $E_\alpha = 8784$  keV,  $T_{1/2} = 0.299$   $\mu\text{s}$ )  $\rightarrow ^{208}\text{Pb}$  ( $^{232}\text{Th}$  family). As two decays in the last (and fast) chain cannot be time-resolved in the  $\text{CaWO}_4$  scintillator (with decay time  $\approx 9$   $\mu\text{s}$ ), they will result in one event registered in the detector. However, because the shape indicator of such an event is different from that for pure  $\alpha$  and  $\beta$  pulses, this component of the detector background was effectively rejected by the pulse-shape analysis. The five counts, remaining in the 3.6–5.4 MeV interval, most probably belong to the  $\beta$  decay of  $^{208}\text{Tl}$ , the contribution of which could be minimized by



Table 3  
Radioactive contaminations in  $\text{CaWO}_4$  and  $\text{CdWO}_4$  [8,23–25] crystal scintillators in the present work

Chain	Nuclide	Activity (mBq/kg)	
		$\text{CaWO}_4$	$\text{CdWO}_4$
$^{232}\text{Th}$	$^{232}\text{Th}$	0.69(10)	0.053(5)
	$^{228}\text{Th}$	0.6(2)	$\leq 0.004\text{--}0.039(2)^a$
$^{235}\text{U}$	$^{227}\text{Ac}$	1.6(3)	0.0014(9)
$^{238}\text{U}$	$^{238}\text{U}$	14.0(5)	$\leq 0.6$
	$^{230}\text{Th}$	—	$\leq 0.5$
	$^{226}\text{Ra}$	5.6(5)	$\leq 0.004$
	$^{210}\text{Pb}$	$\leq 430$	$\leq 0.4$
	$^{210}\text{Po}$	291(5)	—
	$^{40}\text{K}$	$\leq 12$	0.3(1)
	$^{90}\text{Sr}$	$\leq 70$	$\leq 0.2$
	$^{113}\text{Cd}$	—	580(20)
	$^{113m}\text{Cd}$	—	1–30 <sup>a</sup>
	$^{137}\text{Cs}$	$\leq 0.8$	$\leq 0.3\text{--}0.43(6)$
	$^{147}\text{Sm}$	0.49(4)	$\leq 0.04$

<sup>a</sup>In different crystals.

further reducing the  $^{232}\text{Th}$  impurities in the  $\text{CaWO}_4$  crystals. This is certainly feasible.

The summary of the measured radioactive contamination of the  $\text{CaWO}_4$  crystal scintillator (or limits on their activities) is given in Table 3, again in comparison with the  $\text{CdWO}_4$  detectors [8,23–25]. From this comparison one can see that radioactive impurities in the  $\text{CaWO}_4$  crystals (available at present) are much higher (by factor of  $10\text{--}10^3$ ) than those of the  $\text{CdWO}_4$  scintillators.

### 3. Discussion

#### 3.1. $2\beta$ decay of calcium and tungsten isotopes

$\text{CaWO}_4$  crystals contain several potentially  $2\beta$  decaying nuclides which are listed in Table 4. As shown in Ref. [26],  $\text{CaWO}_4$  scintillators provide an excellent opportunity to search for  $0\nu 2\beta$  decay of  $^{48}\text{Ca}$  due to adequate energy resolution and promising background features. The energy resolution FWHM  $\approx 2.9\%$  at the  $Q_{\beta\beta}$  energy of  $^{48}\text{Ca}$  was estimated by fitting the data measured with various  $\gamma$ -ray sources (see Subsection 2.1 and Fig. 1). Despite rather high radioactive contamination,

Table 4  
 $2\beta$  unstable nuclides present in  $\text{CaWO}_4$  crystals

Transition	Mass difference (keV) [32]	Isotopic abundance (%) [19]	Decay channel
$^{40}\text{Ca} \rightarrow ^{40}\text{Ar}$	193.78(0.29)	96.941(0.156)	$2\varepsilon$
$^{46}\text{Ca} \rightarrow ^{46}\text{Ti}$	990.4(2.4)	0.004(0.003)	$2\beta^-$
$^{48}\text{Ca} \rightarrow ^{48}\text{Ti}$	4272(4)	0.187(0.021)	$2\beta^-$
$^{180}\text{W} \rightarrow ^{180}\text{Hf}$	146(5)	0.12(0.01)	$2\varepsilon$
$^{186}\text{W} \rightarrow ^{186}\text{Os}$	488.0(1.7)	28.43(0.19)	$2\beta^-$

the background rate of the  $\text{CaWO}_4$  detector (mass of 189 g) in the energy region 3.6–5.4 MeV, was reduced to the level of 0.07 counts/(yr keV kg) and the half-life limit  $T_{1/2} > 6 \times 10^{19}$  yr at 68% CL was set for the neutrinoless  $2\beta$  decay of  $^{48}\text{Ca}$  [26]. With  $\approx 100$  kg of enriched  $^{48}\text{CaWO}_4$  crystals (assuming their enrichment of about 90%, and radiopurity similar to that of the present  $\text{CdWO}_4$  crystals) the sensitivity in terms of the half-life limit of the  $0\nu 2\beta$  decay is estimated as  $T_{1/2}^{0\nu} \approx 10^{27}$  yr. The latter translates to constraints on the Majorana neutrino mass in the range (0.04–0.09) eV, depending on the nuclear matrix elements calculations used. The proposed technique with the  $^{48}\text{CaWO}_4$  crystal scintillators is very simple and reliable, thus, such an experiment can run stably for decades.

The double-beta processes in the tungsten isotopes were previously searched for with cadmium tungstate crystals [8,27]. Using non-enriched  $\text{CaWO}_4$  detectors, with lower levels of radioactive contamination, the sensitivity to double-beta processes in  $^{180}\text{W}$  and  $^{186}\text{W}$  could be essentially improved comparatively to the previous experiment [8,27] due to the absence of the  $\beta$  active  $^{113}\text{Cd}$  and the  $2\nu 2\beta$  active  $^{116}\text{Cd}$  which are present in  $\text{CdWO}_4$  detectors.<sup>7</sup>

#### 3.2. $\text{CaWO}_4$ crystals as detectors for a dark matter search

$\text{CaWO}_4$  is a promising material for dark matter detection. The reason is that this crystal scintillator can also work as cryogenic detector, and hence,

<sup>7</sup>The contribution from the  $2\nu 2\beta$  decay of  $^{48}\text{Ca}$  with half-life  $\approx 4 \times 10^{19}$  yr [28,29] would be practically negligible taking into account a small isotopic abundance of  $^{48}\text{Ca}$ .

allows one to detect phonon and scintillation light signals simultaneously. The latter could provide a powerful tool for discrimination of the effect (signals of recoil nuclei) from the background events caused by electrons,  $\alpha$  particles, etc. [9,10]. Accordingly, there is an interesting possibility to search for spin-dependent inelastic scattering of WIMPs with excitation of low-energy nuclear levels.  $\text{CaWO}_4$  contains  $^{183}\text{W}$  nuclide ( $\delta = 14.3\%$ ) with a non-zero ground state spin ( $1/2^-$ ) and the first excited state ( $3/2^-$ ) at 47 keV (M1 transition). Therefore, searches for spin-dependent inelastic scattering of WIMPs, with excitation of low-energy nuclear level at 47 keV of the  $^{183}\text{W}$  can be realized by using the cryogenic technique. Identification of “mixed” (nuclear recoil plus  $\gamma$  quanta) events could be possible due to the simultaneous registration of heat and light signals. The heat/light ratio for such events would differ from “pure” nuclear recoil or  $\gamma(\beta)$  events [9,10].

However, the radioactive contamination of the crystals available now (e.g., studied in the present work and in Refs. [9,10]) is rather high, and must be substantially improved. A research and development program has been started, aiming to obtain  $\text{CaWO}_4$  crystals less contaminated. As a first step, we plan to grow  $\text{CaWO}_4$  crystals from raw materials of different producers, and to check their radioactive contamination and background. It should be stressed that the radiopurity level required for  $\text{CaWO}_4$ , has been already achieved with  $\text{CdWO}_4$  [8,23–25] and  $\text{ZnWO}_4$  [30] crystal scintillators. Apparently, the achievement of such a radiopurity will make calcium tungstate detectors (non-enriched isotopically) competitive for dark matter searches.

### 3.3. $\alpha$ decay of $^{180}\text{W}$

An indication of the alpha decay of  $^{180}\text{W}$  (the expected energy of alpha particles is 2460(5) keV, isotopic abundance of  $^{180}\text{W}$  is  $\delta = 0.12\%$ ), with a half-life  $1.1_{-0.4}^{+0.8} \times 10^{18}$  yr, was previously obtained in measurements with low background  $\text{CdWO}_4$  scintillators [14].

A peculiarity in the measured alpha spectrum of the  $\text{CaWO}_4$  detector at the energy 447(8) keV (see

inset (b) in Fig. 6) corresponds to the  $\alpha$  particle energy of 2471(30) keV. These alpha events can be attributed to the  $\alpha$  decay of  $^{180}\text{W}$ . The  $\text{CaWO}_4$  detector contains  $4.7 \times 10^{20}$  nuclei of  $^{180}\text{W}$ . The area of the peak is  $(38 \pm 16)$  counts, which gives, taking into account 59% efficiency of the pulse-shape selection technique,  $(64 \pm 27)$  alpha decays. Thus, the half-life of  $^{180}\text{W}$  obtained in the present experiment is  $T_{1/2} = 1.0_{-0.3}^{+0.7} \times 10^{18}$  yr. This result is in agreement with that published earlier [14] and also with that reported very recently [31], where the alpha decay of  $^{180}\text{W}$  with  $T_{1/2} = 1.8_{-0.2}^{+0.2} \times 10^{18}$  yr has been unambiguously observed with the help of  $\text{CaWO}_4$  cryogenic detector.

## 4. Conclusions

Scintillation properties of the  $\text{CaWO}_4$  crystals were studied. The FWHM energy resolution of 7.2% and 3.8% for the 662 and 2615 keV  $\gamma$ -ray lines was obtained with a  $\text{CaWO}_4$  crystal scintillator placed in a liquid and viewed by two PMTs. Shapes of the scintillation signals were investigated, and distinct pulse-shape discrimination for  $\gamma(\beta)$  and  $\alpha$ -decay events was achieved. Dependences of the  $\alpha/\beta$  ratio and scintillation pulse shape on the energy of alpha particles were measured.

Radioactive contaminations of the  $\text{CaWO}_4$  crystals were determined in the low background set-up installed in the Solotvina Underground Laboratory.  $\text{CaWO}_4$  scintillators are considerably contaminated with uranium and thorium (particularly by  $^{210}\text{Po}$  at the level of  $\approx 0.3$  Bq/kg). However, by applying the developed methods of pulse-shape discrimination and time-amplitude analysis of data, the background rate of the  $\approx 0.19$  kg  $\text{CaWO}_4$  detector in the energy region 3.6–5.4 MeV has been reduced down to 0.07 counts/(keV kg yr). It is one of the lowest background rates ever reached in double beta decay experiments with scintillators or semiconductor detectors. This fact demonstrates the potential of  $\text{CaWO}_4$  crystals for  $2\beta$  decay study of several potentially  $2\beta$  active isotopes of calcium and tungsten, in particular,  $^{48}\text{Ca}$  with the highest  $Q_{\beta\beta}$  energy. The feasibility of a  $0\nu\beta\beta$ -decay

experiment with  $^{48}\text{Ca}$  awaits an efficient and affordable technique of isotopic enrichment of  $^{48}\text{Ca}$ .

The indication for the alpha decay of  $^{180}\text{W}$  was confirmed in the measurements with the  $\text{CaWO}_4$  crystal. The half-life obtained in the present experiment is  $T_{1/2} = 1.0_{-0.3}^{+0.7} \times 10^{18}$  yr.

The  $\text{CaWO}_4$  crystals can also be used for the search of spin-dependent inelastic WIMP scattering on nuclei with nonzero spin (e.g.,  $^{183}\text{W}$ ), which would provide a strong signature of the effect via registration of the nuclear recoil and subsequent low energy  $\gamma$  quanta.

## References

- [1] V.I. Tretyak, Yu.G. Zdesenko, At. Data Nucl. Data Tables 61 (1995) 43;  
V.I. Tretyak, Yu.G. Zdesenko, At. Data Nucl. Data Tables 80 (2002) 83.
- [2] Yu.G. Zdesenko, Rev. Mod. Phys. 74 (2002) 663.
- [3] J.D. Vergados, Phys. Rep. 361 (2002) 1.
- [4] S.R. Elliot, P. Vogel, Annu. Rev. Nucl. Part. Sci. 52 (2002) 115.
- [5] L. Bergstrom, Rep. Prog. Phys. 63 (2000) 793;  
L. Bergstrom, Nucl. Phys. B (Proc. Suppl.) 118 (2003) 329;  
Y. Ramachers, Nucl. Phys. B (Proc. Suppl.) 118 (2003) 341.
- [6] J. Suhonen, O. Civitarese, Phys. Rep. 300 (1998) 123.
- [7] Yu.G. Zdesenko, et al., J. Phys. G: Nucl. Part. Phys. 30 (2004) 971.
- [8] F.A. Danevich, et al., Phys. Rev. C 68 (2003) 035501.
- [9] M. Bravin, et al., Astropart. Phys. 12 (1999) 107.
- [10] S. Cebrián, et al., Phys. Lett. B 563 (2003) 48.
- [11] R.J. Moon, Phys. Rev. 73 (1948) 1210.
- [12] R.H. Gillette, Rev. Sci. Instrum. 21 (1950) 294.
- [13] G.B. Beard, W.H. Kelly, Nucl. Phys. 16 (1960) 591.
- [14] F.A. Danevich, et al., Phys. Rev. C 67 (2003) 014310.
- [15] J.B. Birks, Theory and Practice of Scintillation Counting, Pergamon, London, 1964.
- [16] T. Fazzini, et al., Nucl. Instr. and Meth. A 410 (1998) 213.
- [17] E. Gatti, F. De Martini, Nuclear Electronics 2, IAEA, Vienna, 1962, p. 265.
- [18] Yu.G. Zdesenko, et al., Proceedings of the Second International Symposium on Underground Physics, Baksan Valley, USSR, August 17–19, 1987, Moscow, Nauka, 1988, p. 291.
- [19] K.J.R. Rosman, P.D.P. Taylor, Pure Appl. Chem. 70 (1998) 217.
- [20] R.B. Firestone, et al., (Eds.), Table of Isotopes, eighth ed., Wiley, New York, 1996.
- [21] F.A. Danevich, et al., Phys. Lett. B 344 (1995) 72.
- [22] F.A. Danevich, et al., Nucl. Phys. A 694 (2001) 375.
- [23] A.Sh. Georgadze, et al., Instrum. Exp. Tech. 39 (1996) 191.
- [24] S.Ph. Burachas, et al., Nucl. Instr. and Meth. A 369 (1996) 164.
- [25] F.A. Danevich, et al., Z. Phys. A 355 (1996) 433.
- [26] Yu.G. Zdesenko, et al., Astropart. Phys., submitted for publication.
- [27] F.A. Danevich, et al., Nucl. Phys. A. 717 (2003) 129.
- [28] A. Balysh, et al., Phys. Rev. Lett. 77 (1996) 5186.
- [29] V.B. Brudanin, et al., Phys. Lett. B 495 (2000) 63.
- [30] F.A. Danevich, et al., Nucl. Instr. and Meth. A., to be submitted for publication.
- [31] C. Cozzini, et al., nucl-ex/0408006.
- [32] G. Audi, A.H. Wapstra, Nucl. Phys. A 595 (1995) 409.